Analytical transformed harmonic oscillator basis for continuum discretized coupled channels calculations

A. M. Moro,[1] J. M. Arias,[1] J. Gómez-Camacho,[1,2] and F. Pérez-Bernal[3]

[1]*Departamento de Física Atómica, Molecular y Nuclear, Facultad de Física, Universidad de Sevilla, Apartado 1065, E-41080 Sevilla, Spain*

[2]*Centro Nacional de Aceleradores, Avda Thomas A. Edison, E-41092 Sevilla, Spain*

[3]*Departamento de Física Aplicada, Universidad de Huelva, E-21071 Huelva, Spain*

(Received 7 August 2008; revised manuscript received 14 October 2009; published 16 November 2009)

A new method for continuum discretization in continuum-discretized coupled-channels calculations is proposed. The method is based on an analytic local-scale transformation of the harmonic-oscillator wave functions proposed for other purposes in a recent work [Karataglidis *et al.*, Phys. Rev. C **71**, 064601 (2005)]. The new approach is compared with the standard method of continuum discretization in terms of energy bins for the reactions $d + {}^{58}$Ni at 80 MeV, ^{6}Li + ^{40}Ca at 156 MeV, and ^{6}He + ^{208}Pb at 22 MeV and 240 MeV/nucleon. In all cases very good agreement between both approaches is found.

DOI: 10.1103/PhysRevC.80.054605 PACS number(s): 24.10.Eq, 25.10.+s, 25.45.De

I. INTRODUCTION

For many years, the continuum-discretized coupled-channels (CDCC) method has been the most successful and accurate method for studying nuclear reactions induced by weakly bound projectiles. Although originally designed to account for the effect of the breakup channels in direct nuclear reactions involving deuterons [1–3], it soon proved to be a useful tool to describe reactions induced by other weakly bound nuclei that could be to some extent described within a two-cluster model such as ^{6}Li [4–9] or ^{7}Li [9–13] and, more recently, the scattering of exotic nuclei such as ^{8}B [14–17], ^{7}Be [13], or ^{11}Be [18,19]. The CDCC method has been extended lately to describe the scattering of three-body projectiles and has successfully described the elastic scattering of ^{6}He [20–23].

In the CDCC method, an effective three-body problem is solved approximately via the expansion of the full wave function in a selected set of continuum wave functions of the weakly bound projectile internal Hamiltonian. An essential ingredient of the method is a representation of the projectile continuum in terms of a finite set of internal states. Although not strictly necessary, it is numerically advantageous to use a set of L^2 (i.e., square integrable) functions for this representation. So far, two kinds of discretization methods have been used, namely the bin method and the pseudostate (PS) method. In the former case, the continuum is first truncated by defining a maximum excitation energy of the projectile and then it is divided into a finite set of energy intervals. For each interval, or bin, a representative function is constructed by superposition of true scattering wave functions within that interval (the *average* method, denoted Av hereafter). By construction, the functions obtained in this way are normalizable and mutually orthogonal. In the PS method, by contrast, the wave functions describing the internal motion of the projectile are the eigenstates of the projectile Hamiltonian in a truncated basis of square-integrable functions. A possible election is a harmonic oscillator (HO) basis [24]. The HO is convenient from a computational point of view, although its Gaussian asymptotic behavior is not appropriate to describe the exponentially decaying wave functions associated with weakly bound states.

To overcome this problem, in a series of previous works, we proposed a basis of pseudostates aimed at describing the scattering of two-body composite systems [25–30]. The method provides a discrete representation of the continuum spectrum starting from the ground-state wave function, which is the only required input. A local-scale point transformation (LST) [31,32] that maps this function into the HO ground-state wave function is defined. Once the LST is obtained, the inverse transformation is applied to the HO basis, giving rise to the so-called transformed harmonic oscillator (THO) basis, which is used to represent the continuum (and other bound states if they exist) of the two-body system. The method was first developed in Ref. [25] for simple one-dimensional problems and was later extended to check its applicability and limitations [26–30]. In particular, it was shown in Refs. [17,27] that the combination of the THO discretization method with the coupled-channels technique, named CDCC-THO, can be useful to describe continuum effects in nuclear collisions.

A characteristic feature of the THO method, as formulated in our previous works, is that the eigenvalues resulting from the diagonalization of the projectile Hamiltonian in the PS basis tend to pile up at small excitation energies. This is a direct consequence of the fact that all the basis functions decay with the asymptotic momentum associated with the tail of the ground-state wave function which, for weakly bound systems, is very small. Hence, the THO basis functions have a long range in configuration space or, conversely, a short range in momentum space. This feature can be very convenient in some situations (e.g., in Coulomb-dominated reactions, where the transferred momentum to the projectile is small). However, in cases where high excitation energies are involved, this property may not be desirable because a very large basis might be required to have a sufficient density of states at these excitation energies.

In this paper, we propose an alternative prescription to define the LST, taken from the recent work of Karataglidis

et al. [33]. In that work the authors were interested in the description of the structure of exotic nuclei and their effect in elastic scattering experiments. In their approach, bound single-particle wave functions are required for making a g-folding optical potential. For this purpose, the usual shell-model (HO) orbitals have the problem of lacking the correct asymptotic behavior. Karataglidis *et al.* proposed to keep the simplicity of the HO wave functions, converting their asymptotic behavior to the physical exponential decrease using an analytic LST. The transformed single-particle wave functions are then used as input into calculations of elastic scattering involving the exotic nucleus. We are interested instead in reaction calculations for which a representation of the continuum is needed. The aim of this work is to show that the analytic transformation proposed by Karataglidis *et al.* is very efficient for producing a discrete basis (including both bound and unbound states) suitable for modeling complex reaction problems involving weakly bound nuclei.

Similarly to the LST used in our THO method, the LST proposed in Ref. [33] is applied to the HO basis in such a way that the Gaussian tail is transformed into an exponential. However, the LST proposed by Karataglidis *et al.* is given by an analytic formula and, in general, does not transform the first HO function into the ground state of the system. Therefore, after diagonalization in a finite basis, the ground-state wave function is only approximately obtained. The new LST has two appealing features. First, the basis is very easily generated due to the simple analytic form of the LST. This property is very important for actual calculations because it avoids serious numerical problems when a large number of basis states are generated. Second, and more important, the radial extension of the basis wave functions is controlled by the parameters that define the transformation. In turn, this radial extension determines the energy distribution of the eigenvalues.

The goal of this paper is to show that the THO basis obtained with the analytic LST provides a suitable and efficient representation of the continuum of a two-body system, to be used in CDCC calculations. Results obtained with this representation will be compared with those obtained using the conventional binning procedure for three different reactions.

The paper is organized as follows. In Sec. II the THO method is briefly reviewed. In Sec. III the analytic LST is presented. In Sec. IV we present CDCC calculations in which we compare the standard bin procedure with the new THO prescription for three different reactions: $d + {}^{58}$Ni at 80 MeV, ^{6}Li $+ {}^{40}$Ca at 156 MeV (with special emphasis on the role of the d-wave resonance) and ^{6}He $+ {}^{208}$Pb at 22 MeV and 240 MeV/nucleon. Finally, in Sec. V, the main conclusions of this work are summarized.

II. THE THO METHOD

For completeness, in this section we briefly review the THO approach as formulated in our previous works. Although the method has been recently extended to three-body projectiles [23,34], in this paper we restrict ourselves to the two-body case.

The key idea of the THO method is to construct a basis to describe the states associated with intercluster relative motion. For this purpose, we perform an LST [31,32] on the HO basis. The motivation of this transformation is to correct the asymptotic behavior of the HO basis, converting the Gaussian tail into an exponential, as corresponds to a bound-state wave function in a finite potential. This condition by itself is not sufficient to determine unambiguously the LST. In our previous formulation, we imposed a more restrictive condition by requiring that the ground-state HO wave function is exactly transformed by the LST into the ground state of the system, which is assumed to be known, either analytically or numerically. Mathematically, this condition can be written as

$$\phi_{\mathrm{g.s.},\ell_0}(r) = \sqrt{\frac{ds}{dr}}\,\phi^{\mathrm{HO}}_{0,\ell_0}[s(r)], \tag{1}$$

where $\phi^{\mathrm{HO}}_{0,\ell_0}(s)$ is the radial part of the HO wave function for the orbital angular momentum ℓ_0 expressed in the dimensionless variable s, and $\phi_{\mathrm{g.s.},\ell_0}(r)$ is the ground-state wave function of the two-body system. The subscript ℓ_0 represents the intercluster relative angular momentum. To simplify the notation, we do not consider the intrinsic spins of the fragments.

Once the $s(r)$ function has been obtained, the THO basis is generated by applying the same LST calculated for the ground state to the rest of the HO wave functions. Because of the simple analytical structure of the HO wave functions, this is equivalent to multiplying the ground-state function by the appropriate Laguerre polynomial $L_n^{\ell+1/2}(s)$ [27]:

$$\phi^{\mathrm{THO}}_{n,\ell}(r) = [s(r)]^{\ell-\ell_0} L_n^{\ell+1/2}[s(r)^2]\phi_{\mathrm{g.s.},\ell_0}(r). \tag{2}$$

Notice that, by construction, the family of functions $\phi^{\mathrm{THO}}_{n,\ell}(r)$ is orthogonal and constitutes a complete set. Moreover, these functions decay exponentially at large distances, thus ensuring the correct asymptotic behavior for the bound wave functions. In practical calculations a finite set of functions (2) are retained, and the internal Hamiltonian of the projectile is diagonalized in this truncated basis, giving rise to a set of eigenvalues and their associated wave functions. As the basis size is increased, those eigenstates with negative energy will tend to the exact bound states of the system, whereas eigenstates with positive eigenvalues can be regarded as a finite representation of the unbound states. Note that, due to the particular choice of the LST, the ground state of the system is exactly recovered for any basis size.

By construction, all basis functions (2) decay asymptotically with the same functional dependence as the ground-state wave function, namely, $\sim\exp(-k_{\mathrm{g.s.}}r)$, with $k_{\mathrm{g.s.}} = \sqrt{2\mu|\varepsilon_{\mathrm{g.s.}}|}/\hbar$, where μ is the reduced mass of the two clusters. For weakly bound systems, this produces states with a large radial extension or, equivalently, with a short range in momentum space. Consequently, the eigenstates obtained by diagonalization of the internal Hamiltonian in a finite THO basis tend to concentrate at small excitation energies. The basis so obtained is then particularly suitable to describe excitations to the low-lying continuum, such as Coulomb-dominated reactions [17].

However, in situations in which higher excitation energies are involved, one may need to use a large THO basis to obtain

enough density of states at high excitation energies and, hence, the THO discretization may not be so efficient. Moreover, the range of excitation energies that will be effectively populated depends on the specific reaction. Thus, it would be desirable to develop an alternative definition of the LST in which the radial extension of the basis functions can be optimized according to the problem under consideration. At the same time, it would be desirable to keep the most appealing properties of the LST transformation, namely, (i) at small distances, the LST should be such that the radial dependence of the HO functions is not modified and, (ii) asymptotically, the Gaussian behavior should be transformed to an exponential dependence in the physical variable r.

III. THE ANALYTIC LST

Recently, an analytic LST that meets the requirements cited earlier has been proposed and used for problems related to nuclear structure [33]. This LST is given by the expression

$$s(r) = \frac{1}{\sqrt{2}b}\left[\frac{1}{\left(\frac{1}{r}\right)^m + \left(\frac{1}{\gamma\sqrt{r}}\right)^m}\right]^{\frac{1}{m}}, \tag{3}$$

which depends on the parameters m, γ, and the oscillator length b.[1] It can be easily verified that the function $s(r)$ behaves asymptotically as $s(r) \sim \frac{\gamma}{b}\sqrt{\frac{r}{2}}$ and, hence, the functions obtained by applying this LST to the HO basis behave at large distances as $\exp(-\gamma^2 r/2b^2)$. Thus, one can define an effective momentum, $k_{\rm eff} = \gamma^2/2b^2$, that governs the asymptotic behavior of the THO functions. The quantity $k_{\rm eff}$ can be interpreted as the range of linear momentum that is *explored* by the THO basis. This interpretation suggests that, for a reaction that excites states in the continuum up to a maximum energy $\varepsilon_{\rm max}$, the value of $k_{\rm eff}$ should be of the order of $\sqrt{2\mu\varepsilon_{\rm max}}/\hbar$. This determines completely the ratio γ/b. Note that the parameter $k_{\rm eff}$ plays a role similar to that of the maximum momentum used in the standard binning method to truncate the continuum. As a second step, the oscillator length b is determined by minimizing the ground-state energy with respect to this parameter for a finite size basis. Thus, the quantity b can be regarded as a variational parameter used to optimize the description of the ground-state wave function. With this procedure, we completely determine b and γ. Concerning the power m, we have found that the results are very weakly dependent on this parameter and, hence, in this work we take $m = 4$, which is in fact one of the choices used in Ref. [33].

[1]Note that this definition contains the extra factor $(\sqrt{2}b)^{-1}$ with respect to the original definition of Ref. [33]. This extra factor arises because in the present work the HO functions are defined in terms of the dimensionless variable s, whereas in Ref. [33] they are defined in dimensional units. Hence, unlike the original definition, the oscillator length appears explicitly in the definition used in this work.

IV. NUMERICAL APPLICATIONS OF THE ANALYTIC LST

A. $d + {}^{58}$Ni at 80 MeV

As a first application of the method, we consider the reaction $d + {}^{58}$Ni at 80 MeV, which has been the subject of many studies in the past [3,35–37]. Following our previous work [27], the proton-neutron (pn) interaction is parametrized in terms of the Poeschl-Teller potential,

$$V_{pn}(r) = -\frac{V_0}{\cosh(ar)^2}, \tag{4}$$

with $V_0 = 102.706$ MeV and $a = 0.9407$ fm^{-1}. As explained earlier, the ratio of the γ parameter to the oscillator length is estimated as $\gamma/b \simeq \sqrt{2k_{\rm eff}}$, where $k_{\rm eff}$ is the linear momentum associated with the maximum excitation energy populated in the reaction. In this case, we find that states up to about 70 MeV are excited, which corresponds to $k_{\rm eff} = 1.3$ fm^{-1} and $\gamma/b = 1.65$ fm$^{-1/2}$. Keeping this ratio fixed, the oscillator length is then determined by minimizing the energy of the lowest eigenvalue obtained upon diagonalization of the projectile Hamiltonian in a small THO basis, in this case giving $b = 1.5$ fm. Nevertheless, it is worth noting that the scattering calculations are found to be weakly sensitive to the actual choice of this parameter.

As an example, in Fig. 1 we plot the positive eigenvalues obtained for $\ell = 0$ with a basis of $N = 20$ states. The vertical scale corresponds to the linear momentum for the internal motion (i.e., $k = \sqrt{2\mu\varepsilon}/\hbar$). For the sake of comparison, we include also the spectrum obtained with our previous prescription for the LST, in which the transformation $s(r)$ is determined by imposing the condition that the first ($n = 0$) HO wave function is transformed into the ground-state wave function of the system. (The latter was obtained by direct integration of the Schrödinger equation.) Note that, unlike the analytical LST, the numerical LST is independent of oscillator

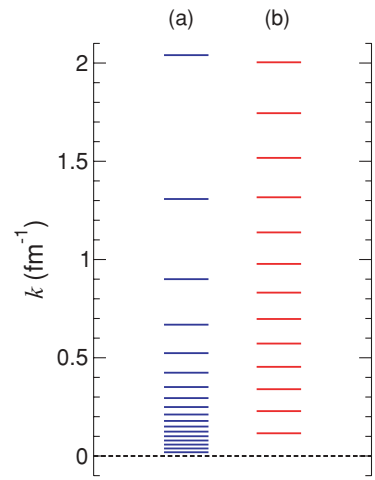

FIG. 1. (Color online) Eigenvalues of the pn system obtained upon diagonalization of the internal Hamiltonian (a) using a THO basis generated with the numerical LST based on the ground-state wave function and (b) using a THO basis generated with the analytical LST of Eq. (3). A basis with $N = 20$ functions was used in both cases. Only eigenvalues below $k = 2.1$ fm^{-1} are shown.

length. It can be seen in the numerical LST, Fig. 1(a), that the eigenvalues tend to concentrate at low excitation energies. This is mainly because in this case the exponential decay of the THO basis is determined by the asymptotic momentum of the ground state ($k_{\text{g.s.}} = 0.232$ fm^{-1}). In the analytical LST, Fig. 1(b), the basis functions decay with the momentum $k_{\text{eff}} = 1.3$ fm^{-1}, as explained earlier, and the eigenvalues are approximately equally distributed in momentum space. Besides these positive eigenvalues, both bases produce a negative eigenvalue which, in the case of the numerical LST, coincides by construction with the exact ground-state energy ($\varepsilon_{\text{g.s.}} = -2.225$ MeV). In the analytical LST, the ground-state energy and its associated wave function are obtained only approximately, but with $N = 20$ states the lowest eigenvalue is $\varepsilon_{\text{g.s.}} = -2.225$ MeV and the overlap between the exact and the approximate ground-state wave functions is 0.999998, indicating that the ground state obtained with the analytical transformation reproduces very well the exact one for even a relatively small basis set.

Within the CDCC formalism, the set of eigenstates is used to generate the coupling potentials (diagonal and nondiagonal) between different internal states of the projectile. For $d + {}^{58}$Ni, these coupling potentials are given by[2]

$$U_{\alpha,\alpha'}(\mathbf{R}) = \langle \phi_{n,\ell} | U_{p\text{-Ni}} + U_{n\text{-Ni}} | \phi_{n',\ell'} \rangle, \tag{5}$$

with $\alpha = \{n, \ell\}$ and $\alpha' = \{n', \ell'\}$ and $U_{p,n\text{-Ni}}$ are the nucleon-target interactions (in the proton case, including Coulomb interaction). The internal wave functions $\phi_{n,\ell}(r)$ in this formula represent either the continuum bins or the THO eigenstates, depending on the selected discretization method. In the present calculations, the proton-^{58}Ni and neutron-^{58}Ni interactions are taken from the parametrization of Becchetti and Greenless [38]. Following Ref. [3], we consider only the partial waves $\ell = 0, 2$. All possible couplings (s-s, s-d, and d-d) were included in the calculations for multipoles $\lambda \leqslant 4$. In the standard CDCC calculation, the $\ell = 0$ and $\ell = 2$ continuum was discretized into $n_s = n_d = 15$ bins evenly spaced in the linear momentum and up to a maximum excitation energy of $\varepsilon_{\text{max}} = 70$ MeV.

For the CDCC-THO calculations we used a basis with $N = 30$ states (for each ℓ). After diagonalization, some of the eigenvalues lie at very high excitation energies, thereby playing a negligible role in the studied observables. In particular, in this calculation we excluded those eigenstates above 70 MeV, because they were found to have no effect on the elastic cross section. After removal of these channels, the number of states that are included is reduced to $n_s = n_d = 14$ (plus the ground state).

The coupled equations were solved for total angular momenta up to $J_{\text{max}} = 100$ and integrated up to a radius $R_{\text{max}} = 100$ fm.

In Fig. 2 we compare the differential elastic cross section obtained with CDCC-Av (solid line) and CDCC-THO (dashed line) with the experimental data of Stephenson *et al.* [39] for $d + {}^{58}$Ni at 79 MeV. It can be seen that both methods are in very good agreement, proving the independence of these

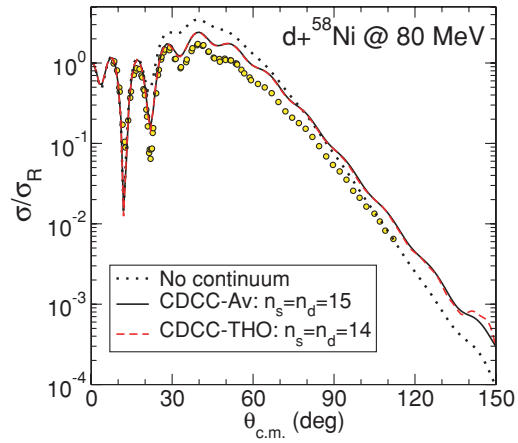

FIG. 2. (Color online) Elastic angular distribution, relative to the Rutherford cross section, for the reaction $d + {}^{58}$Ni at 80 MeV. The solid line corresponds to the CDCC calculation with bin discretization, the dashed line to the CDCC-THO calculation, and the dotted line to the one-channel calculation, in which continuum channels are neglected. The variables n_s and n_d denote the number of continuum states included in the CDCC calculations for $\ell = 0$ and $\ell = 2$, respectively. The circles are the experimental data of Ref. [39].

calculations with respect to the discretization method. For comparison, we include also in this figure the one channel calculation in which continuum channels are omitted (dotted line). It is observed that, at this energy, the effect of the coupling to the continuum on the elastic cross section is sizable and that the inclusion of these couplings significantly improves the agreement with the experimental data, with respect to the one-channel calculation.

The solution of the coupled equations also provides the S-matrix elements connecting the ground state with the continuum states, from which breakup observables can be constructed. In principle, each matrix element corresponding to a given set of quantum numbers would be a continuous function of the excitation energy (or momentum). However, within a coupled-channels scheme, the S matrix is obtained for discrete values of the energy. In the standard CDCC method, in which this discretized continuum is represented by continuum bins, an approximation to this continuous S matrix can be obtained dividing the discrete S matrix by the square root of the bin width, Δk_i. In the CDCC-THO method, one could apply a similar procedure by assigning a width to each pseudostate. In fact, this approach was used in Ref. [27] to calculate the differential breakup cross section from the cross section to individual pseudostates, assuming that the width of the ith pseudostate is given approximately by $\Delta_i = (\varepsilon_{i+1} - \varepsilon_{i-1})/2$. In this work, we adopt an alternative approach, previously proposed in Ref. [7] and recently employed in a previous application of the THO method [17]. In this method, the breakup S-matrix elements $S_{\alpha':\alpha}(k)$, which depend on both the continuous variable k and the initial and final angular momenta, are obtained by an appropriate superposition of the discrete S-matrix elements $\hat{S}_{\alpha':\alpha}(k_i)$ resulting from the solution

[2]In this expression, the integral is along the internal coordinate **r**.

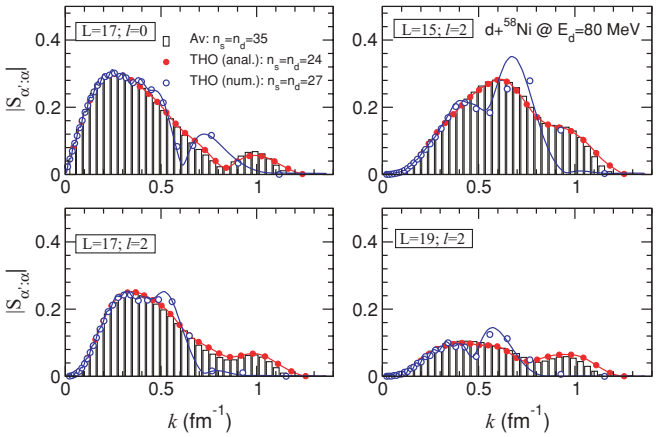

FIG. 3. (Color online) Modulus of the breakup S-matrix elements for the total angular momentum $J = 17$ for the reaction $d + {}^{58}$Ni at 80 MeV as a function of the p-n relative momentum in the final state. The histogram is the CDCC calculation with binning method. The filled and open circles represent the CDCC-THO calculations using the analytical and numerical LSTs, respectively. The solid lines are obtained by folding the discrete S matrices with the *true* continuum wave functions.

of the coupled-channels equations, as [7,15]

$$S_{\alpha':\alpha}(k) \approx \sum_{i=1}^{N} \langle \phi^{(s)}_{k,\ell} | \phi_{i,\ell} \rangle \hat{S}_{\alpha':\alpha}(k_i), \tag{6}$$

where $\phi^{(s)}_{k,\ell}(r)$ is the true scattering wave function for the partial wave ℓ and energy $\varepsilon = \hbar^2 k^2/2\mu$. The sum runs over the set of pseudostates included in the coupled-channels calculation. The indexes α and α' denote the initial and final channels; that is, $\alpha = \{\text{g.s.}; L_0, \ell_0, J\}$ and $\alpha' = \{i; L, \ell, J\}$, where L_0 (L) is the initial (final) orbital angular momentum for the projectile-target relative motion.

As an example, in Fig. 3 we plot the modulus of the breakup S-matrix elements for a total angular momentum of $J = 17$; that is, $(\ell, L) = (0, 17), (2, 15), (2, 17), (2, 19)$. For the CDCC-Av calculations, the continuum was divided into $n_s = n_d = 35$ bins up to a maximum excitation energy of 70 MeV. For the CDCC-THO calculation, we required a basis of $N = 50$ states to obtain full convergence at high excitation energies, although $N = 30$ already gives rather good results. Again, after diagonalization of the internal Hamiltonian, we removed those eigenstates above 70 MeV, reducing the actual size of the basis to only $n_s = n_d = 24$ states (along with the ground state). The histogram in Fig. 3 represents the CDCC-Av calculation; the filled circles correspond to the CDCC-THO calculation, in which each discrete S matrix has been divided by the square root of the pseudostate width; and the line is the CDCC-THO calculation folded with the continuum wave functions, Eq. (6). We verified that increasing the number of basis states does not change the calculated S matrices, thus indicating the convergence of the THO method with respect to the basis size. It is clearly seen that both discretization methods are in almost perfect agreement. To illustrate the advantage of the present LST over the previous one, we have included in Fig. 3 the calculation using the numerical transformation, with a basis of $N = 30$ states (open circles). After eliminating those pseudostates above 70 MeV, the number of states included in the CDCC calculation is reduced to $n_s = n_d = 27$ states. It can be seen that this calculation gives a distribution very similar to the other methods at low excitation energies, where the density of states is higher, but it clearly deviates from them at higher excitation energies. We attribute this departure to the small number of states at these energies.

B. ^{6}Li + ^{40}Ca at 156 MeV

The second example presented in this work corresponds to the scattering of ^{6}Li from ^{40}Ca at an incident energy of 156 MeV. The ^{6}Li nucleus is assumed here to be composed of two fragments, $\alpha + d$, as has usually been done in previous studies (see, for example, Refs. [6–9]). An important difference with respect to the deuteron case is the presence of a d-wave resonance in the ^{6}Li continuum. This feature permits an assessment of the extent to which our THO basis is capable of reproducing the effect of this resonance on scattering observables.

This reaction was recently studied by Matsumoto *et al.* [7] as a test case to compare the binning method with a PS method based on a family of Gaussian functions, and very good agreement was found between both discretization methods for both elastic and breakup observables. With a similar motivation, in this work we performed CDCC calculations for this reaction, comparing the binning procedure with the THO basis. The ^{6}Li ground-state wave function was calculated with the same Gaussian potential used in Ref. [7], assuming a $2S$ configuration and a separation energy of 1.474 MeV. The same potential was used to generate the continuum wave functions. For $\ell = 2$, this potential produces a resonance with $\varepsilon_{\text{res}} = 2.96$ MeV and $\Gamma = 0.62$ MeV. Only the partial waves $\ell = 0$ and $\ell = 2$ were considered for the $\alpha + d$ relative motion. The optical potentials for the fragment-target interactions ($\alpha + {}^{40}$Ca and $d + {}^{40}$Ca) were also taken from Ref. [7]. These interactions were used to generate the coupling potentials (diagonal and nondiagonal) for multipoles $\lambda \leqslant 2$, including both nuclear and Coulomb parts. For simplicity, the deuteron spin was ignored.

In the CDCC-Av calculations, the continuum was truncated at an excitation energy of $\varepsilon_{\max} = 80$ MeV. For $\ell = 0$, this energy interval was divided into $n_s = 15$ bins uniformly distributed in the linear momentum. For $\ell = 2$, we considered $n_d = 30$ bins distributed in the following way: ten bins from $\varepsilon = 0$ up to an excitation energy of $\varepsilon = 5$ MeV, and 20 bins from this energy to $\varepsilon_{\max}$. This was done to have a finer description of the region around the resonance. Moreover, for the interval $\varepsilon \in [0, 5]$ MeV, the bin wave functions were built as usual by superposition of the true continuum states, but with a weight function $\sin(\delta_k)$, where δ_k is the phase shift corresponding to an asymptotic momentum k for the α-d relative motion. This weight factor is known to improve the description of the resonance.

The THO basis was generated following the same procedure employed in the preceding example but without any fine tuning due to the presence of the resonance. In this case, the

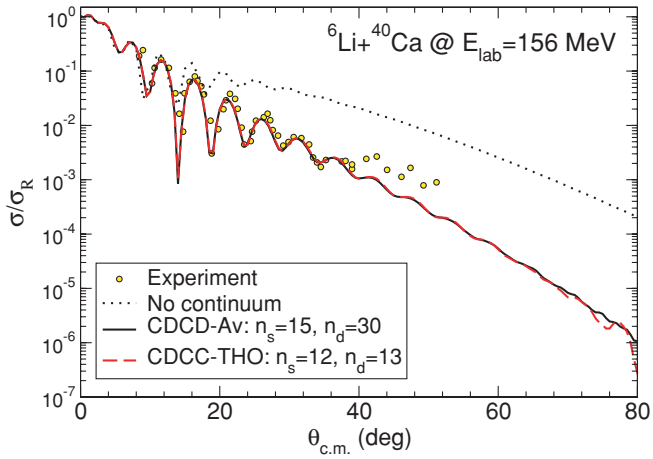

FIG. 4. (Color online) Elastic angular distribution, relative to the Rutherford cross section, for the reaction ^{6}Li + ^{58}Ni at 156 MeV. The dotted line is the calculation omitting the breakup channels, the solid line is the CDCC-Av calculation, and the dashed line is the CDCC-THO calculation. Experimental data are from Ref. [40].

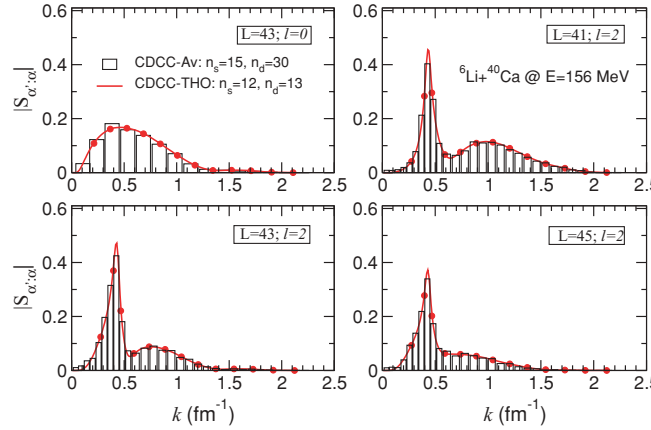

FIG. 5. (Color online) Breakup S-matrix elements for the reaction ^{6}Li + ^{40}Ca at 156 MeV, for a total angular momentum of $J = 43$ as a function of the final $d + \alpha$ relative linear momentum.

maximum energy populated is about 80 MeV, which yields $k_{\max} = 2.26$ fm^{-1} and $\gamma/b = 2.13$ fm$^{-1/2}$. The oscillator parameter was obtained by minimizing the binding energy in a small THO basis, giving $b \simeq 2$ fm. For the coupled-channels calculations, a basis of $N = 20$ was used. When the projectile Hamiltonian is diagonalized in this basis, the ground-state energy differs from the exact value by less than 0.1% and the overlap of its eigenfunction with the exact ground-state wave function is 0.999996, showing again the good accuracy of the approximated ground state obtained with the analytic transformation. We note that a deeply bound eigenvalue is also obtained at $\varepsilon = -33.5$ MeV. This corresponds to the $1S$ configuration that is forbidden due to the Pauli principle; hence, this state was excluded from our calculations. We also excluded those eigenstates above 80 MeV, reducing the actual basis dimension to $n_s = 12$ (plus the ground state) and $n_d = 13$ states. The set of coupled equations was solved for a total angular momentum up to $J_{\max} = 150$ and matched to their asymptotic solution at $R_{\max} = 150$ fm.

In Fig. 4 we present the elastic cross section, relative to the Rutherford cross section, for the CDCC-Av (solid line) and CDCC-THO (dashed line) calculations, along with the experimental data from Ref. [40]. The single-channel calculation, in which the continuum is omitted, has also been included (dotted line). From this figure, one can see that, except for the very small differences observed at large scattering angles (where the cross section is already very small), each discretization method yields almost identical results. Despite the simplified model for the ^{6}Li spectrum, the full CDCC calculations also reproduce the experimental data very well.

In Fig. 5 we compare the modulus of the breakup S-matrix elements for a total angular momentum of $J = 43$. The histogram corresponds to the CDCC-Av calculation, the circles to the CDCC-THO calculation obtained by dividing the discrete S-matrix elements by the square root of the pseudostate widths, and the solid line to the CDCC-THO calculation in which the discrete values are folded with the true continuum states, according to Eq. (6). Again, we find excellent agreement between both discretization methods. The most remarkable feature of this quantity is the presence of a prominent peak at $k = 0.44$ fm^{-1} for the $\ell = 2$ continuum, which arises from the d-wave resonance. It is clearly seen that this peak is very well described by the THO discretization (even before folding with the continuum states). Therefore, we can conclude that the THO basis is also an efficient procedure to describe the resonant continuum and its effect on the scattering observables.

C. ^{6}He + ^{208}Pb at 22 MeV and 240 MeV/nucleon

As a final example, we consider the reaction ^{6}He + ^{208}Pb at 22 MeV and 240 MeV/nucleon. These two energies are chosen to illustrate how the basis can be adapted to the different energy regimes by an appropriate choice of the parameters that define the LST.

We first focus on the reaction at 22 MeV. This case is very demanding because of (i) the strong couplings arising from the long-range Coulomb interaction and (ii) the proximity of the incident energy to the Coulomb barrier, making both nuclear and Coulomb effects very important.

The ^{6}He system is treated within the two-body model proposed in Ref. [41]. This is analogous to the $\alpha + d$ model used for the ^{6}Li system, but with an effective dineutron binding energy of 1.6 MeV, instead of the two-neutron separation energy ($\varepsilon_b = 0.97$ MeV). This modification provides a more realistic rms value for the ground-state wave function, in addition to more realistic couplings to continuum states. Following Ref. [41], the $2n$-α interaction is parametrized with a Woods-Saxon shape, with $R = 1.9$ fm and $a = 0.25$ fm. The strength of the $\ell = 0$ potential is adjusted to give a separation energy of 1.6 MeV. For the $\ell = 2$ continuum states, we use the same geometry but with the strength adjusted to give a 2^+ resonance at an excitation energy of 1.8 MeV (with respect to the ground state).

To generate the LST, we considered a maximum momentum $k_{\max} = 0.72$ fm^{-1} (corresponding to a maximum excitation

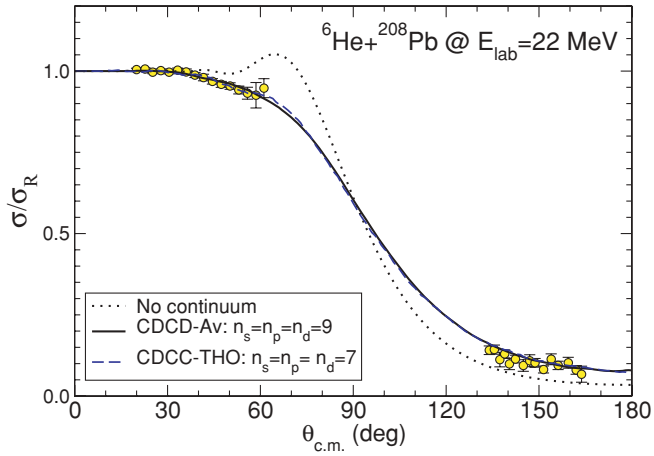

FIG. 6. (Color online) Elastic angular distribution, relative to the Rutherford cross section, for the reaction $^6\mathrm{He} + {}^{208}\mathrm{Pb}$ at 22 MeV. The solid line corresponds to the CDCC calculation with bin discretization, the dashed line to the CDCC-THO calculation, and the dotted line to the single-channel calculation, in which continuum channels are neglected. The circles are the experimental data of Ref. [44].

energy of 8 MeV), which leads to $\gamma/b = 1.2$ fm$^{-1/2}$. With this ratio, the value of the oscillator length that minimizes the binding energy is $b \simeq 1$ fm. For the scattering calculations, we considered $\ell = 0$, 1, and 2 continuum states. Unlike the preceding examples, the role of the $\ell = 1$ continuum states is very important because these states are strongly coupled by the dipole Coulomb interaction. In the three cases, we used a basis of $N = 15$ states, providing the ground-state energy with an accuracy of 1.25% and an overlap with the exact wave function of 0.999868. At this incident energy, we found that the elastic scattering is not affected by the continuum states above ≈8 MeV. Therefore, those pseudostates with eigenenergies above this value were not included in the solution of the coupled equations. After removing these states, the number of pseudostates actually included were $n_s = n_p = n_d = 7$.

Again, we compare the CDCC-THO calculations with CDCC-Av calculations using the binning method. In this case, we discretize the s, p, and d continuum using nine bins, uniformly distributed in the linear momentum from $\varepsilon = 0$ to $\varepsilon = 9$ MeV.

For the $2n$-^{208}Pb interaction we used the d-^{208}Pb potential generated with the global parametrization of Perey and Perey [42], whereas for the $\alpha + {}^{208}$Pb interaction we took the optical potential of Barnett and Lilley [43]. The coupled equations were integrated up to a radius of 100 fm and for total angular momenta up to $J_{\max} = 100$.

In Fig. 6 we compare the experimental data for the differential elastic cross section of Ref. [44] (circles) with the CDCC-Av calculation (solid line) and the CDCC-THO calculation (dashed line). Both calculations are in excellent agreement and reproduce the data very well. To emphasize the effect of the coupling on the continuum, we have also represented the result obtained by omitting the continuum contribution (dotted line). The strong suppression of the cross section around 70° is mainly due to the strong dipole Coulomb couplings with 1^- continuum states. Given the good agreement between both discretization methods, we conclude that the THO method is also suitable to describe the effects caused by long-range couplings.

In Fig. 7 we present the breakup S-matrix elements for a total angular momentum of $J = 29$, for which the breakup cross section is largest. To achieve convergence in the calculations of this observable, the coupled equations had to be integrated to $R_{\max} = 700$ fm. In addition, the number of states used in both discretization methods had to be increased. For the CDCC-THO calculation (solid circles), we used a basis of

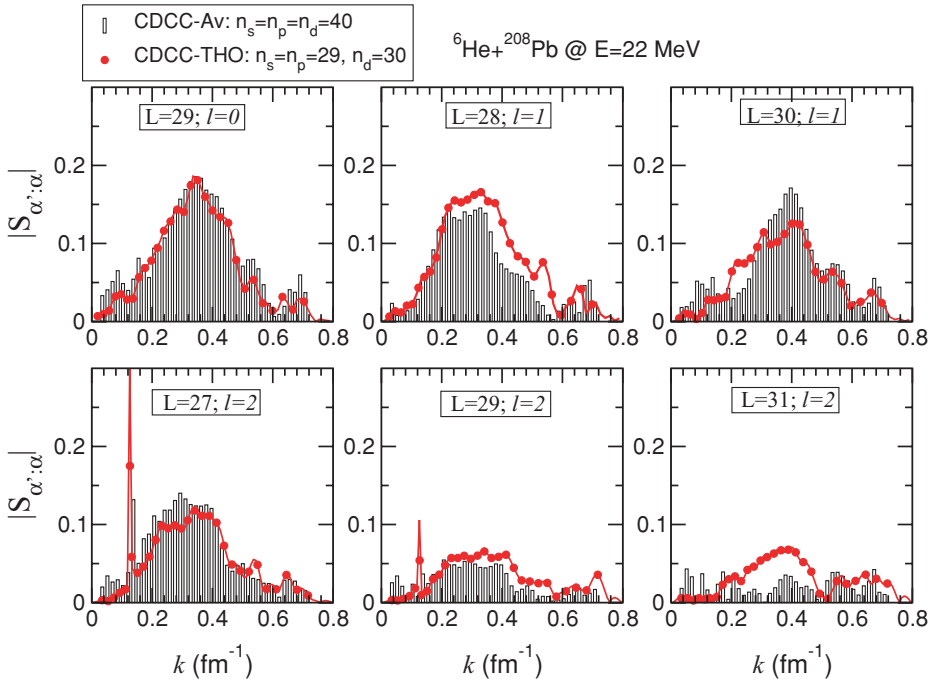

FIG. 7. (Color online) Breakup S-matrix elements for the reaction $^6\mathrm{He} + {}^{208}\mathrm{Pb}$ at 22 MeV, for a total angular momentum of $J = 29$ as a function of the α-$2n$ relative momentum in the final state. The histogram is the CDCC-Av calculation, whereas the filled circles and the solid line correspond to the CDCC-THO calculations.

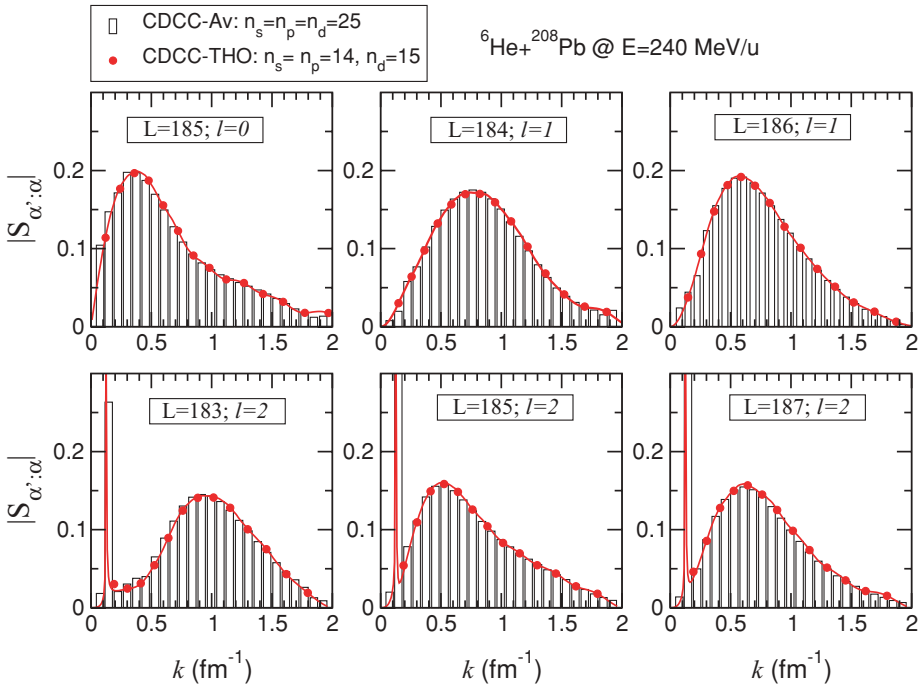

FIG. 8. (Color online) Breakup S-matrix elements for the total angular momentum of $J = 185$ for the reaction ^{6}He + ^{208}Pb at 240 MeV/nucleon as a function of the final $2n$-α relative momentum. The histogram is the CDCC calculation with the binning method. The circles represent the CDCC-THO calculations using the analytic LST and the solid lines are obtained by folding the discrete S matrices with the *true* continuum wave functions.

$N = 50$ states. After eliminating those states above 8 MeV, the number of pseudostates per partial wave was reduced to $n_s = n_p = 29$ and $n_d = 30$ states. The panels for $\ell = 2$ final states show a narrow peak at low energies, which corresponds to the well-known 2^+ resonance. This peak becomes more evident when the discrete S matrix is folded with the continuum wave functions (solid line). For the CDCC-Av method, we used a basis with $n_s = n_p = n_d = 40$ bins. For this observable, the CDCC-Av calculation was found to be very sensitive to the radius at which the bin wave functions are truncated ($r_{\rm bin}$). We have chosen the criterion $r_{\rm bin} = 2\pi/\Delta k$, where Δk is the bin width. This value of $r_{\rm bin}$ corresponds to the distance at which all continuum wave functions exhibit a common minimum.

The results shown in Fig. 7 show a reasonably good agreement between both discretization methods, although, for the excitation to the dipole states, differences as large as 25% are found between them. This difference is larger than the accuracy estimated for the calculated S matrices (about 10%), so this disagreement requires further investigation.

Finally, we consider the same reaction but at the much higher energy of $E_{\rm lab} = 240$ MeV/nucleon. We use the same internal Hamiltonian for the ^{6}He system and, for simplicity, we keep the same $2n$-target and α-target interactions. Although the large available kinetic energy would allow the population of very high excited states, in practice states up to only about 60 MeV are significantly populated. This corresponds to $k \simeq 2$ fm^{-1} and, according to our prescription, $\gamma/b = 2$ fm$^{-1/2}$.

For the CDCC-THO calculations, very good convergence of this observable was achieved with a basis of $N = 30$ states. Excluding those eigenstates above 60 MeV, the number of pseudostates that enter the coupled-channels equations is $n_s = n_p = 14$ and $n_d = 15$. For the CDCC-Av method, the continuum was discretized from 0 up to 50 MeV, using $n_s = n_p = n_d = 25$ bins evenly spaced in the linear momentum. The coupled equations were integrated up to 100 fm, and for a total angular momentum up to $J_{\rm max} = 2000$.

In Fig. 8 we depict the breakup S-matrix elements for a total angular momentum of $J = 185$, which corresponds to the maximum of the breakup cross section. As before, the histogram is the CDCC-Av calculation, and the circles and the solid lines are the CDCC-THO calculations. In the latter case, the breakup S matrices are folded with the continuum wave functions. Excellent agreement is observed in all cases, but the CDCC-THO method required a smaller basis to achieve convergence. Note that this smoothing procedure permits an accurate description of the 2^+ resonance, even with a small number of pseudostates. From these results, we conclude that the proposed discretization method can be useful for the analysis of high-energy experiments involving weakly bound projectiles.

V. SUMMARY AND CONCLUSIONS

In this work, we proposed a new transformed oscillator basis for continuum discretization in CDCC calculations. This new THO basis is obtained by application of a recently proposed LST [33] to the HO basis. The basis obtained provides a suitable discrete representation of the bound and unbound spectrum of a two-body system, which can be used within the CDCC formalism to calculate the scattering observables for reactions involving weakly bound projectiles. Unlike the THO used in our previous works, this analytic transformation does not provide the exact ground-state wave function for any finite size of the basis, but in the cases studied in this work we have shown that the energy and wave function of the ground state can be obtained with high accuracy using a relatively small basis dimension. An appealing feature of this

transformation is that the radial extension of the basis can be controlled with the parameter γ defining the transformation and the oscillator length b. This flexibility is very convenient for scattering calculations, because it permits adaptation of the distribution of eigenvalues to the problem at hand. Moreover, it can be very easily implemented, due to its analytic form. This fact is important in realistic calculations for which a large basis set is needed, because the generation of any number of states is straightforward with the analytic LST, whereas numerical problems appear when generating a large-dimension basis if the numerical LST developed in previous works is used.

As an application of the new basis, we have studied the elastic and breakup of $d + {}^{58}$Ni at 80 MeV, ^{6}Li + ^{40}Ca at 156 MeV, and ^{6}He + ^{208}Pb at 22 MeV and 240 MeV/nucleon, showing in most cases excellent agreement with the standard discretization method based on energy bins. Furthermore, typically the number of states required to achieve converged results in the CDCC-THO calculations is smaller than the number of bins included in the CDCC-Av calculations. This is a clear advantage of the present method. Even the sharp resonance peak that appears in the ^{6}Li + ^{40}Ca and ^{6}He + ^{208}Pb breakup energy distributions is very well described using a relatively small basis. In the ^{6}He + ^{208}Pb case, we have shown that the THO method accounts very well for the effect of long-range Coulomb couplings. In this case, the convergence rate has been found to be significantly faster than that of the CDCC-Av method. For this reaction, we have performed calculations at $E_{\rm lab} = 22$ MeV and 240 MeV/nucleon to illustrate how the basis can be adapted to the energy dynamic regime by a suitable choice of parameters for the LST. At $E_{\rm lab} = 22$ MeV, we have found excellent agreement for the differential elastic cross section between both methods, whereas for the breakup S-matrix elements, differences as large as 20% have been observed. This discrepancy should be further investigated. At $E_{\rm lab} = 240$ MeV/nucleon, these differences were not observed, and the two methods provide almost identical results for this magnitude.

Finally, we note that the present method could be extended to describe the continuum of a three-body projectile, such as ^{6}He or ^{11}Li, following the same formalism used in Ref. [23]. Moreover, the method can be useful to study the continuum structure of two- and three-body systems with no bound states. Work in this direction is in progress.

ACKNOWLEDGMENTS

This work was partially supported by the Spanish Ministerio de Educación y Ciencia and by the European regional development fund (FEDER) under Project Nos. FIS2008-04189 and FPA2006-13807-c02-01 and by the Spanish Consolider-Ingenio 2010 Programme CPAN (CSD2007-00042). A.M.M. and F.P.B. acknowledge financial support from the Junta de Andalucía.

[1] R. C. Johnson and P. J. R. Soper, Phys. Rev. C **1**, 976 (1970).
[2] G. H. Rawitscher, Phys. Rev. C **9**, 2210 (1974).
[3] N. Austern, Y. Iseri, M. Kamimura, M. Kawai, G. Rawitscher, and M. Yahiro, Phys. Rep. **154**, 125 (1987).
[4] Y. Sakuragi, M. Yahiro, and M. Kamimura, Prog. Theor. Phys. (Kyoto) **70**, 1047 (1983).
[5] Y. Sakuragi, M. Kamimura, S. Micek, H. Rebel, and H. J. Gils, Z. Phys. A **322**, 627 (1985).
[6] Y. Sakuragi, Phys. Rev. C **35**, 2161 (1987).
[7] T. Matsumoto, T. Kamizato, K. Ogata, Y. Iseri, E. Hiyama, M. Kamimura, and M. Yahiro, Phys. Rev. C **68**, 064607 (2003).
[8] K. Rusek, N. Alamanos, N. Keeley, V. Lapoux, and A. Pakou, Phys. Rev. C **70**, 014603 (2004).
[9] C. Beck, N. Keeley, and A. Diaz-Torres, Phys. Rev. C **75**, 054605 (2007).
[10] N. J. Davis *et al.*, Phys. Rev. C **52**, 3201 (1995).
[11] I. Martel, J. Gómez-Camacho, K. Rusek, and G. Tungate, Nucl. Phys. **A641**, 188 (1998).
[12] K. Rusek, P. D. Cathers, E. E. Bartosz, N. Keeley, K. W. Kemper, and F. Marechal, Phys. Rev. C **67**, 014608 (2003).
[13] N. Keeley, K. W. Kemper, and K. Rusek, Phys. Rev. C **66**, 044605 (2002).
[14] F. M. Nunes and I. J. Thompson, Phys. Rev. C **59**, 2652 (1999).
[15] J. A. Tostevin, F. M. Nunes, and I. J. Thompson, Phys. Rev. C **63**, 024617 (2001).
[16] T. Egami, K. Ogata, T. Matsumoto, Y. Iseri, M. Kamimura, and M. Yahiro, Phys. Rev. C **70**, 047604 (2004).
[17] A. M. Moro, F. Pérez-Bernal, J. M. Arias, and J. Gómez-Camacho, Phys. Rev. C **73**, 044612 (2006).
[18] M. Takashina, S. Takagi, Y. Sakuragi, and Y. Iseri, Phys. Rev. C **67**, 037601 (2003).
[19] N. C. Summers and F. M. Nunes, Phys. Rev. C **76**, 014611 (2007).
[20] T. Matsumoto, E. Hiyama, M. Yahiro, K. Ogata, Y. Iseri, and M. Kamimura, Nucl. Phys. **A738**, 471 (2004).
[21] T. Matsumoto, E. Hiyama, K. Ogata, Y. Iseri, M. Kamimura, S. Chiba, and M. Yahiro, Phys. Rev. C **70**, 061601(R) (2004).
[22] T. Matsumoto, T. Egami, K. Ogata, Y. Iseri, M. Kamimura, and M. Yahiro, Phys. Rev. C **73**, 051602(R) (2006).
[23] M. Rodríguez-Gallardo, J. M. Arias, J. Gómez-Camacho, R. C. Johnson, A. M. Moro, I. J. Thompson, and J. A. Tostevin, Phys. Rev. C **77**, 064609 (2008).
[24] A. U. Hazi and H. S. Taylor, Phys. Rev. A **1**, 1109 (1970).
[25] F. Pérez-Bernal, I. Martel, J. M. Arias, and J. Gómez-Camacho, Phys. Rev. A **63**, 052111 (2001).
[26] F. Pérez-Bernal, I. Martel, J. M. Arias, and J. Gómez-Camacho, Few-Body Syst. Suppl. **13**, 217 (2002).
[27] A. M. Moro, J. M. Arias, J. Gómez-Camacho, I. Martel, F. Pérez-Bernal, R. Crespo, and F. M. Nunes, Phys. Rev. C **65**, 011602(R) (2001).
[28] I. Martel, F. Pérez-Bernal, M. Rodríguez-Gallardo, J. M. Arias, and J. Gómez-Camacho, Phys. Rev. A **65**, 052708 (2002).
[29] F. Pérez-Bernal, I. Martel, J. M. Arias, and J. Gómez-Camacho, Phys. Rev. A **67**, 052108 (2003).
[30] M. Rodríguez-Gallardo, J. M. Arias, and J. Gómez-Camacho, Phys. Rev. C **69**, 034308 (2004).
[31] M. V. Stoitsov and I. Z. Petkov, Ann. Phys. (NY) **184**, 121 (1988).

[32] I. Z. Petkov and M. V. Stoitsov, *Nuclear Density Functional Theory, Oxford Studies in Physics* (Clarendon, Oxford, 1991).
[33] S. Karataglidis, K. Amos, and B. G. Giraud, Phys. Rev. C **71**, 064601 (2005).
[34] M. Rodríguez-Gallardo, J. M. Arias, J. Gómez-Camacho, A. M. Moro, I. J. Thompson, and J. A. Tostevin, Phys. Rev. C **72**, 024007 (2005).
[35] M. Yahiro, Y. Iseri, H. Kameyama, M. Kamimura, and M. Kawai, Prog. Theor. Phys. Suppl. **89**, 32 (1986).
[36] R. A. D. Piyadasa, M. Kawai, M. Kamimura, and M. Yahiro, Phys. Rev. C **60**, 044611 (1999).
[37] A. Deltuva, A. M. Moro, E. Cravo, F. M. Nunes, and A. C. Fonseca, Phys. Rev. C **76**, 064602 (2007).
[38] F. D. Becchetti and G. W. Greenlees, Phys. Rev. **182**, 1190 (1969).
[39] E. J. Stephenson, C. C. Foster, P. Schwandt, and D. A. Goldberg, Nucl. Phys. **A359**, 316 (1981).
[40] Z. Majka, H. J. Gils, and H. Rebel, Z. Phys. A **288**, 139 (1978).
[41] A. M. Moro, K. Rusek, J. M. Arias, J. Gómez-Camacho, and M. Rodríguez-Gallardo, Phys. Rev. C **75**, 064607 (2007).
[42] C. M. Perey and F. G. Perey, Phys. Rev. **132**, 755 (1963).
[43] A. R. Barnett and J. S. Lilley, Phys. Rev. C **9**, 2010 (1974).
[44] A. M. Sánchez-Benítez *et al.*, Nucl. Phys. **A803**, 30 (2008).